우주 추진을 위한 Lab-on-PCB: 소형위성 군집화를 위한 추력기의 새로운 제조방법

Lab-on-PCB for space propulsion: New fabrication method of solid propellant micro thruster array f or micro satellite constellation

초록

본 연구에서는 PCB와 일체화 된 고체 추진제 마이크로 추력기의 개념과 제작 공정을 제시하여, 추진 시스템과 위성 전자 제어 시스템의 완전한 통합 가능성을 보여주었다. 이는 Lab-on-PCB 컨셉을 적용 한 하드웨어 및 조립 공정으로 적용하여 3 × 3개의 추력 요소를 가지는 추력기를 제작하여 검증하였다. 핵심 부품인 PCB 연소실 층은 고체 추진제와 마이크로 점화기의 탑재 및 전기적 제어가 용이하게 특수설계 되었다. 핵심 공정인 고체 추진제 탑재 및 마이크로 점화기 제작 기법은 PCB SMT 공정을 차용하여 수행 후 성능 및 업스케일링 가능성을 평가하였다. 상기 두 공정은 대면적화 및 대량 생산에도 적용 가능성이 높다. 제작된 추력기는 여러 회의 연소실험을 통해 점화 및 추진 성능을 검증하였다.

Key Words : Lab-on-PCB, Coating, MEMS thruster, Micro-igniter, Solid propellant

1. 서 론

With the development of small satellite technologies by ever-improving semiconductors[1], markets using them are also on the rise[2]. On account of simple structures and suitability for mass production of small satellites, their operation in constellations is economically and technically propitious[3, 4]. Constellations of small satellites can be used for missions such as earth observation[5, 6] and space missions[7], replacing larger satellites. More importantly, “space internet” has attracted attention as a next-generation network with global coverage for 5G and self-driving[8], and constellations of small satellites arose as a feasible approach.

Forming a satellite constellation requires a lengthy mission lifespan of individual satellites, attitude and orbital control[9], and de-orbit functionalities[10]. These requirements necessitate an actuator to be used in space named satellite thrusters[11, 12]. Still, satellite thrusters designed for micro/nanosatellites (< 10 kg) are in the early development stage, and commercialized thrusters do not meet the technical requirements[13]. Commercialized thrusters contain excessive volume and mass budget[14] for nanosatellites of the most common sizes of 3 U and 6 U[15]. For this reason, only 6.4% of all micro/nanosatellites in orbit[16] contain thrusters, and the number of nanosatellite constellations is currently minimal. The absence of thrusters plays a serious impediment for satellites to meet the requirements to be operated into constellations; thus, microthrusters have been actively developed.

Recently, research in microthrusters has been divided into several fields due to the development of MEMS technology. Conventional thrusting methods using cold gas[17, 18], monopropellants[19-21], or bipropellants[22, 23] have been investigated, not to mention the recent efforts in newer concepts, namely free molecular micro-resistojets[24], plasmas[25, 26], electrosprays[27], and colloid microthrusters[28]. However, conventional methods require an additional volume and mass budget to store liquid propellants or pressurized fluids, and methods based on electricity do not fit nanosatellites given their high power consumption[16]. In contrast, solid propellant micro thruster (SPMT)s have the advantages of simple structure, low power consumption, and high thrust reliability[29-31], together with its feasibility to be applied for small satellites owing to its fitness in downsizing by packaging.

A typical SPMT is composed of micro nozzles, ignitors, combustion chambers, and propellants. The ignitors are undoubtedly the most crucial component for initiating and stable combustion. Commonly, a joule heater is placed on a supporting membrane. In the early stages of SPMT development, indirectly

heating the propellant using a polysilicon or metal heater patterned on a few μm thick silicon membranes was widely adopted[32–34], but the heater could be easily damaged from diminutive outer impacts[35]. Since a rapid manufacturing process requires ignitors with robust mechanical properties, there have been efforts to sputtering metal electrodes onto glass membranes[35, 36]. Nevertheless, the lower heat conductivity and irregular thickness worsened the ignition delay. Recently, a method of patterning the heater below the membrane for it to make direct contact with the propellant was proposed for improved structural stability and ignition delay[37].

Despite the extensive efforts by researchers, multiple difficulties should be tackled before SPMTs can be applied to satellites. Most SPMTs fabricated using the MEMS technology share the limitations of the complicated fabricating process, a limited selection of materials, and inappropriateness for mass production[38]. The limitations are exceptionally prominent for ignitors, which play a critical role and require a more precise manufacturing process. Silicon and glass, materials commonly used for SPMTs, are prone to cracks by internal pressure and impacts during combustion due to their inherent brittleness [21, 39].

We expect that the problems above can be successfully addressed by applying the lab-on-PCB (Printed circuit board) technology, which recently attracted great attention from multiple fields. The lab-on-PCB technology is similar to conventional MEMS or lab-on-Chip technology but differs in using widely commercialized PCB processes and products[40, 41]. A wide range of materials can be used in PCB processes, and the most widely used epoxy board is mechanically robust to outer impacts and vibrations. Also, it is suitable for upscaling since the standardized PCB process allows low-cost and precise manufacturing of integrated microfluidic and electronic platforms[42–44].

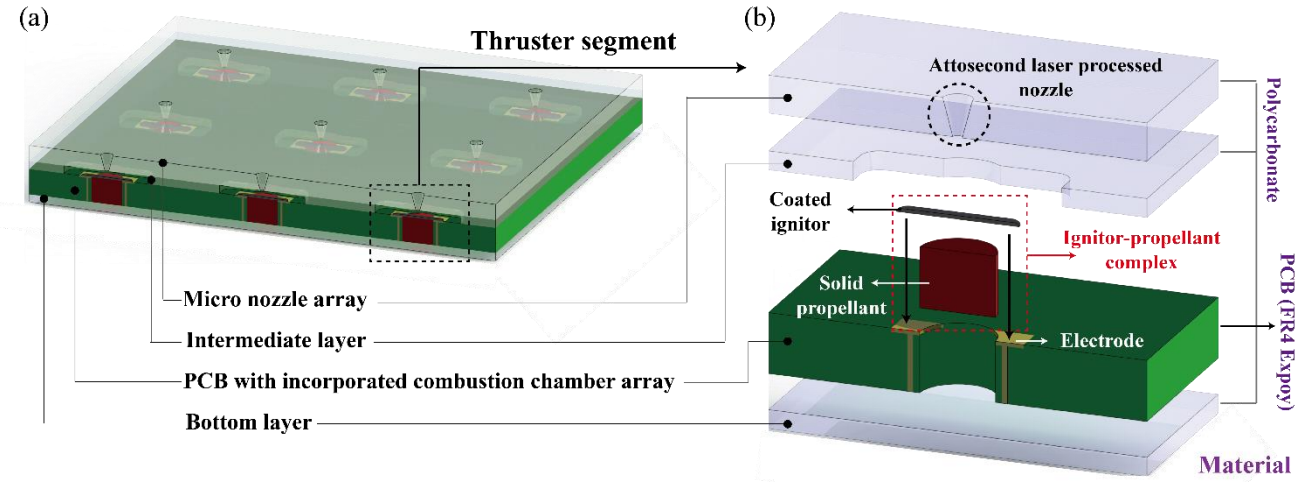

Fig. 1. (a) Schematic of the 3 × 3 SPMT array, (b) Core processes and specific components of the solid propellant micro thruster segment.

In this study, we propose a new method to fabricate a 3 × 3 SPMT array composed of 4 layers using the lab-on-PCB concept (Fig. 1, 2) and evaluate its performance and reliability. We listed the specific processes and materials in Fig. 1(b) that are improved to conform better for mass production and upscaling. The nozzle array was fabricated using a precise and fast attosecond pulse laser. All of the layers that consist of the SPMT are polymers and are resistant to mechanical and thermal shock. We specially designed the PCB with an incorporated combustion chamber array as an on-board thruster for the solid propellant and ignitors to be conveniently installed. The solid propellant was inserted into the PCB combustion chamber using the silkscreen method, and the micro ignitors were applied onto both the solid propellant and the electrodes at the same time to form an ignitor-propellant complex. Our study is the first to report a PCB with incorporated combustion chambers and micro ignitors in the field of microthrusters using chemical propellants. We verified its ignition and thrust performance through a number of combustion experiments.

2. Architecture design

Solid propellant MEMS thrusters can be subcategorized into two types: horizontal types in which all of the main components (nozzles, ignitors, and combustion chambers) are placed on a single layer[45], vertical types in which individual layers of each component are stacked[46, 47]. In order to solve the “one shot of thrust problem” and increase the packaging density, we chose the vertical type with a PCB combustion chamber layer.

The 3 × 3 SPMT array is composed of 4 layers (Fig. 1, 2). Photographs of each layer and its thicknesses can be found in Fig. 2. The PCB layer was made of conventional FR-4 (fiberglass-reinforced epoxy laminate material), and all other layers were made from polycarbonate. All layers share the dimensions of 30 × 30 mm and the hole distance of 10 mm. The first layer is the micro nozzle array, and the second layer separates the ignitor from the nozzle and serves as a post chamber for the combustion gas to reside. The PCB with an incorporated combustion chamber array is the most crucial component and is placed on the third layer. The last and bottom layer seals the propellant chamber. The operating principle is as follows. When the surface temperature of the ignitor-propellant complex reaches the ignition temperature, combustion starts. The high-pressure and high-temperature gas resulting from the combustion of the propellants passes the intermediate layer and is accelerated by the micro nozzles, resulting in thrust.

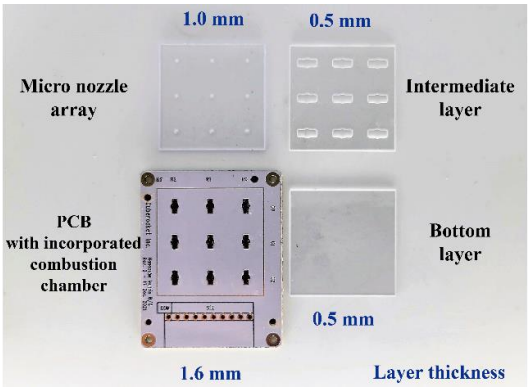

Fig. 2. Four fabricated layers composing a solid propellant micro thruster array

3. Components fabrication

3.1. PCB integrated combustion chamber array

The overall structure of the hardware and the circuitry for electric control could be simplified by applying the lab-on-PCB approach. The PCB was designed by a specialized design tool (PDAS VX.1, Mentor Graphics, USA) and was fabricated by a PCB fabrication service (JLCPCB, china) (Fig. 3(a)). The PCB is composed of a mechanically and thermally durable and shock-resistant FR-4 material. The PCB with an overall thickness of 1.6mm has a multi-layer structure considering attaching to other layers (Fig. 3(b)). Since the exposure of the traces causes protrusion and might hinder proper adhesion between layers, we embedded the circuitry on layer 2 and layer 3 using via holes to improve flatness. We used electroless nickel immersion gold (ENIG) to prevent oxidized layers from forming. To enhance the adhesivity, we coated a 20 μm thick layer of typical white solder resist epoxy. To supply electricity to the conductive paste that acts as ignitor precursors, the copper layer in layer 1 was moved to form electrodes with the size of 4.0 mm × 1.5 mm. Via holes with a diameter of 2.0 mm were drilled at the center of each electrode. This divides each electrode into two with opposite polarities, and the holes act as combustion chambers for the propellant to be inserted. A terminal (colored box in Fig. 3(a)) with multiple pins is located on the board to only ignite selected segments, and copper circuitry with a thickness of 17.5 μm and width of 300 μm connecting the terminal to the electrodes is placed on layer 2 and layer 3. Power is applied to the electrode by the via holes that connect all layers. Electricity enters

from the red box and line, passes through the ignitor, and exits through the blue box and line, in Fig 3a and 3b.

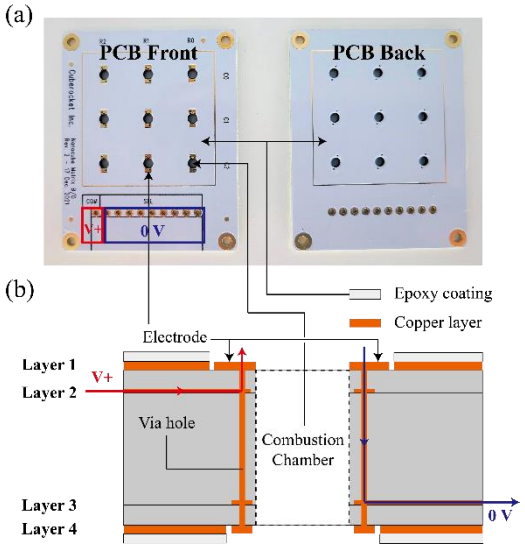

Fig. 3. (a) Front/Back photos of the PCB with incorporated combustion chamber array, (b) Cross-section schematic of a thruster segment.

3.2. Propellant filling process

We were able to achieve fast and even filling of the propellant to the PCB with incorporated combustion chamber by using the surface mount technology (SMT) for PCB, which is commonly used when applying solder paste onto PCBs. In the previous studies, propellants in powder form or with high viscosity were manually inserted. This method might be feasible for research purposes but is not applicable for mass production. In this section, we developed a new propellant filling process and propellant with adequate viscosity for stencil printing with properties suitable for postprocessing and curing processes.

Chemical propellants are composed of two key ingredients: oxidizer and fuel. In this study, we used ammonium perchlorate (AP) for oxidizer and polydimethylsiloxane, PDMS (Sylgard 184, Dow Inc., USA) for fuel and binder. For base and curing agent for PDMS was mixed at a ratio of 10:1 in weight, for 30 s at 2000 rpm (clockwise), and then 30 s at 2200 rpm (counterclockwise) using a centrifugal mixer (ARE-310, Thinky USA Inc., Laguna Hills, CA). We repeated the same method 3 times to mix the PDMS and AP at a ratio of 1:4 in weight. The resulting propellant had a density of 1.05 g/cm3 and viscosity of 00 Pas with an ignition temperature of 300℃.

Figure 4(a) shows the process of filling the propellant precursor to the PCB described in Section 3.1. The fabricated PCB and stencil to be used were cleaned with isopropyl alcohol and then completely dried with compressed air (Fig. 4(a1)). Kapton tape was attached to the backside of the PCB board to prevent the propellant precursor from flowing down during the stencil process. Then, small holes were made with a needle to allow the air mixed in the filling process to escape the pressure from compression (Fig. 4(a2)). Prior to filling the propellant, the PCB and the 100 um thick stainless steel stencil were aligned and fixed with a supporter (Fig. 4(a3), 4(b)). The filling process (Fig. 4(a4)) was performed with a stencil printer used for solder printing (Fig. 4(b)). The specific process is as follows. First, the squeegee blade with 20 g of propellant precursor is advanced at a fixed speed of 20 mm/s, maintaining a constant pressing force and an angle of 30° to the stencil. In this process, the propellant precursor in a viscous fluid state is filled into the combustion chambers of the PCB. To improve the packaging density, the blade was cleaned and then used to slowly wipe the surface of the metal stencil in the opposite direction to the original direction at 10 mm/s and with an angle of 45°. After repeating the above process twice, the process was again performed twice, this time starting from the opposite side

of the board to fill in the propellant completely. Next, the stencil was removed with caution, and the propellant precursor protruding upward due to the stencil's thickness was removed using a knife (Fig. 4(a5)). Finally, the PCB with incorporated propellant was heated in a convection oven at 150°C for 15 minutes and at 100°C for 60 minutes to cure the propellant (Fig. 4(a6)).

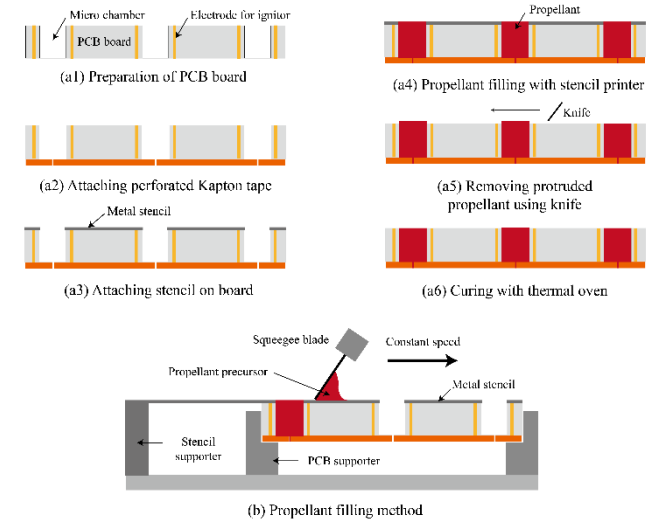

Fig. 4. (a) Process of filling AP/PDMS propellant precursor in a PCB with incorporated combustion chamber, (b) Filling process using a stencil printer

3.3. Ignitor coating process

In this study, our goal is to overcome the limitations of the existing SPMT micro ignitors by using solid propellant with incorporated ignitors. The dielectric-based membrane micro ignitor, which has been mainly studied in the past, is not suitable to mass-produce and upscale and is evaluated as structurally unstable due to its fragility[35]. The requirements that a micro ignitor must achieve for the commercialization of SPMTs include high structural stability, low manufacturing cost in addition to low ignition energy and ignition delay[48, 49]. In this section, a novel fabrication process for a robust micro ignitor is proposed by using the bar-coating technique and stencil techniques in combination. Its feasibility and the potential for upscaling were evaluated.

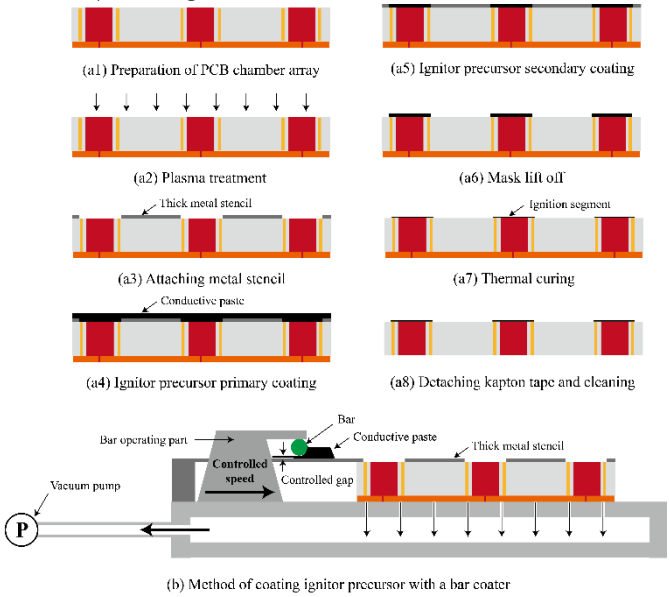

Fig. 5. (a) Fabrication process of the coated micro ignitor, (b) Coating method of conductive paste using a bar coater

In Fig. 5(a), the process of forming micro ignitors on the PCB with incorporated combustion chamber with propellant discussed in Section 3.2 is illustrated. Conductive carbon nanotube (CNT) paste (AccuPaste 25, Bioneer, Korea) with a maximum operating temperature of 320°C was used as the ignitor precursor. We used the bar-coating method, in which the coating thickness is governed by the advancing speed of the bar and the gap between the substrate and the bar (Fig. 5(b)). The micro ignitor fabrication process is as follows. First, the PCB surface was cleaned with isopropyl alcohol and an air compressor (Fig. 5(a1)). Plasma surface treatment was performed on the PCB to improve the adhesion between the conductive paste and the AP/PDMS propellant (Fig. 5(a2)). This was performed for 75 seconds at a power of 100 W and 50 kHz under an oxygen partial pressure of 700 torrs. A polished stainless steel stencil was used to coat the conductive paste on the desired area accurately. The stencil had a relatively thick thickness of 300 μm, and the geometry of the coating slots was designed for the ignitors to have a stable amount of resistance with sufficient length to make proper contact with the copper electrodes on both sides of the combustion chamber hole (3.5 mm × 1.0 mm). After aligning the PCB and the stencil (Fig. 5(a3)), the vacuum pump of the bar coater in Fig. 5(b) creates a negative pressure to fix the board. Since coating in a single step is insufficient to achieve acceptable surface quality due to high viscosity of the conductive paste, the process was performed in two steps as the following. After applying enough conductive paste to the bar of the bar coater, the bar was set to be 75 μm apart from the stencil and was advanced at a uniform speed of 5 mm/s to form the primary coating layer (Fig. 5(a4)). After washing the bar and adjusting the gap to 5 um, it was advanced at 2.5 mm/s in the opposite direction to the initial direction, so that the conductive paste layer almost matched the thickness of the stencil (Fig. 5(a5)). The stencil was carefully removed to minimize the loss of paste (Fig. 5(a6)). Finally, the PCB coated with conductive paste was sintered in a convection oven at 200°C for 120 minutes to result in coated ignitors (Fig. 5(a7)). The thickness of the sintered conductive paste was reduced to 35 μm. It is followed by removing the Kapton tape attached to the backside and cleaning to complete the PCB with incorporated combustion chamber array (Fig. 5(a8)).

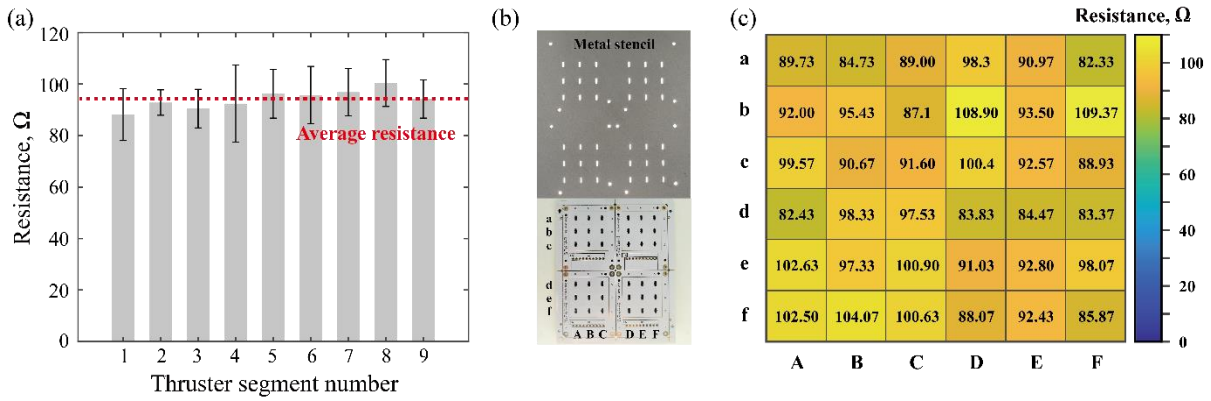

Fig. 6. (a) Resistance of micro ignitor of each segment of the 3 × 3 SPMT array, (b) 6 × 6 SPMT array coated with conductive paste (right) and a metal stencil used for ignitor coating (left), (c) Heatmap graph for resistance distribution of the 6 × 6 micro ignitor array

In order to evaluate the heat generation characteristics and the reliability of the process of the micro ignitors, the resistance of the ignitors of 5 sets of 3 × 3 SPMT array was measured and is shown in Fig. 6a. The average and standard deviation of the resistance were 94.15 Ω and 3.68 Ω, respectively, which were reasonably uniform considering the thrusters were on a feasibility test stage. Therefore, it can be inferred that a nearly consistent amount of heat is transferred from each micro ignitor segment to the solid propellant when it is joule heated with the same applied voltage. As seen in Fig. 6b, stainless steel stencil was used to fabricate the ignitors of a 6 × 6 SPMT array. Using this allowed an experimental validation of its expansion potential to thrusters with larger sizes. In Fig. 6(c), the measured resistance of the ignitors of the 6 × 6 SPMT array is expressed through a heatmap graph. It has a generally uniform resistance value, with an average of 93.52 Ω and a standard deviation of 7.41 Ω. The stencil and PCB were fixed by pressing force, and it could be difficult to distribute the load evenly for larger thrusters

and might result in gaps where insufficient loads were applied. If the conductive paste creeps into this part, ignitors with undesired resistance can be created. In order to expand the process to thrusters with larger areas, it is necessary to control the quality by using equipment with higher precision.

3.4. Nozzle fabrication

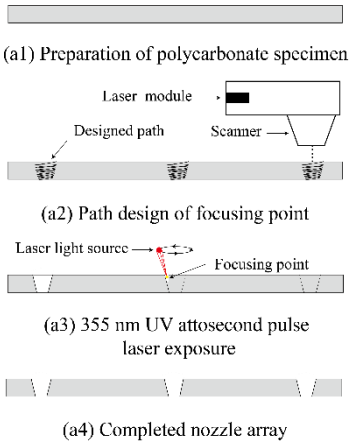

Fig. 7. Fabrication process of the micro nozzle.

The micro nozzle layer was fabricated using an attosecond pulse laser. We used this method because precise and tapered cuts are possible. The detailed procedure is as follows. A polycarbonate specimen was prepared (Fig. 7(a1)), and an optimized path for the laser focus was determined using a scanner installed in the equipment. The inputted geometry of the nozzle is 200.00 μm, 735.90 μm for the nozzle throat and exit, respectively, and the diverging angle was set to be 15° to qualify as a de-Laval nozzle. The machining was performed by attosecond laser pulses with a wavelength of 355 nm along the predetermined path. The average diameter of the 9 nozzle throats was measured to be 200.34 μ m and 740.77 μm for the exits, and the average diverging angle was measured to be 15.12°.

4. Assembly of the thruster array

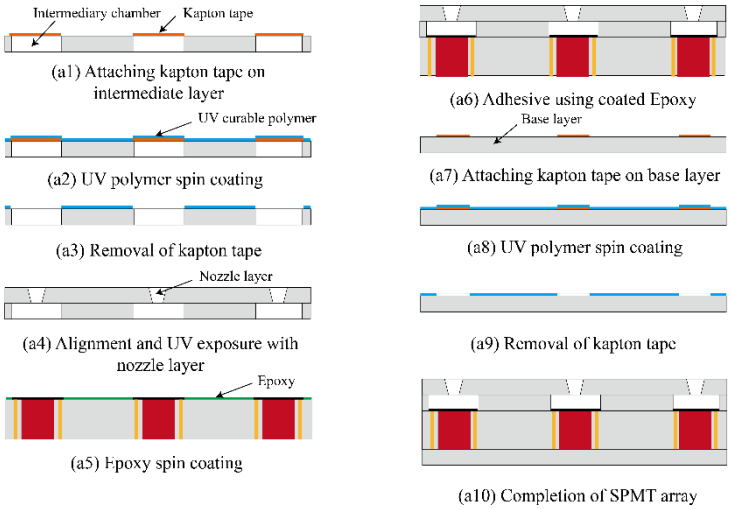

Fig. 8. Assembly process of the SPMT array

The following covers the process of integrating the 4 layers (see Fig. 2) consisting of the SPMT. As can be seen in Fig. 8. the assembly process starts by attaching the nozzle array to the intermediate layer. The intermediate layer was cleaned using isopropyl alcohol and was dried by blowing compressed air. The holes on the 0.5 mm thick intermediate layer were designed to avoid interference with the coated

ignitors. The shape of the holes is a combination of a rectangle with a length of 5.5 mm and a depth of 2 mm with rounded corners of R0.50 and a circle with a diameter of 2.5 mm at its center (see the intermediate layer in Fig. 1(b)). Kapton tape was applied on top of the holes to prevent adhesives from flowing in (Fig. 8(a1)). It is followed by spraying 25 mL of high-temperature-resistant UV curable epoxy (UV-6502CL, Epoxyset, USA) to evenly wet the surface and spin-coating at 600 rpm for 15s to form a uniformly thick layer (Fig. 8(a2)). Then, the Kapton tape was carefully removed using a tweezer (Fig. 8(a3)) and the layer was aligned and attached to the nozzle array (Fig. 8(a4)). Here, we applied uniform pressure to avoid air bubbles by using a pressing zig made with a z-axis stage. The pressing zig was put into an oven that has a 6 W UV lamp installed, and the two layers were rigidly attached by repeating the following process 3 times: shedding light for 1 minute at a 100 mm distance and cooling at room temperature for 1 minute. The cooling was to avoid the thermal deformation of the layers made out of polymers. The next step is attaching the nozzle array complex to the PCB combustion chamber layer. In this process, we used 25 mL of thermally curable epoxy (EB-107LP-1, Epoxyset, USA) with poor wettability to PDMS. The base and the curing agent of the thermally curable epoxy were mixed at a ratio of 4:1 and were wetted on the top surface of the PCB, followed by a spin-coating process at 1000 rpm for 7 s. We created a membraneless micro ignitor by intentionally not performing any plasma treatments to prevent AP/PDMS propellant and the ignitors on top from being wetted by the epoxy (Fig. 8(a5)). The nozzle array complex was aligned to the PCB and was applied force by the pressing zig. At room temperature, the epoxy was cured for 48 hours (Fig. 8(a6)). Attaching the base layer follows a similar process. Kapton tape was attached to the points where the propellant was located (Fig. 8(a7)), and 25 mL of UV curable epoxy was evenly applied, followed by a spin-coating process at 600 rpm for 15 s (Fig. 8(a8)). After removing the Kapton tape (Fig. 8(a9)), the SPMT array is completed by the same process as above: attaching the layer to the bottom part of the PCB and curing it with UV light (Fig. 8(a10)).

5. Testing performance and reliability

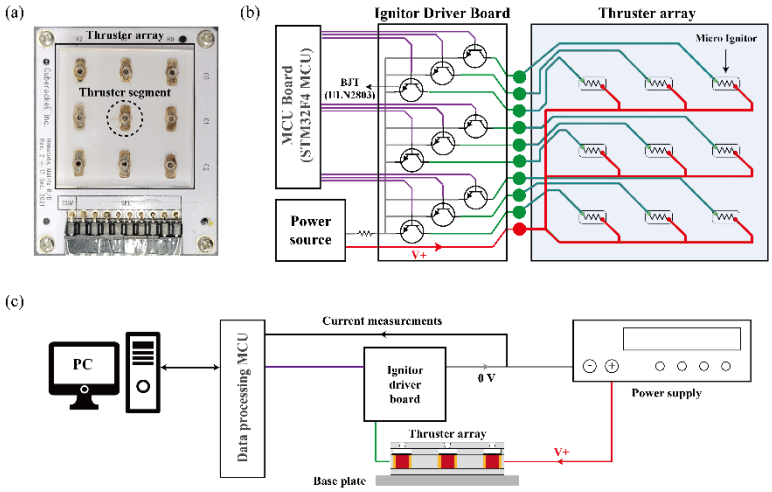

Fig. 9. (a) Assembled SPMT array, (b) PCB internal wiring and control circuit schematic for ignition control, (c) Experiment setup for ignition characteristics and thrust measurement.

The completed SPMT array consists of a total of 9 thruster segments (Fig. 9(a)). An electronic control system was constructed to generate thrust at each segment independently at desired timing(Fig. 9(b)). An ignitor driver board containing a micro-control unit (MCU) and a bipolar junction transistor (BJT) was used. The MCU (STM32F429ZI, STMicroelectronics, Switzerland) determines the ignition timing by controlling the NPN BJT connected to the electrode of each thruster segment. Under atmospheric pressure, a combustion test was carried out to determine the ignition characteristics and thrust of the SPMT. Figure 9(c) shows the experiment setup and measurement equipment. With a voltage divider and a shunt resistor, the voltage/current provided to the igniter was monitored in real-time, and the ignition

delay and ignition energy were measured. We observed the exhausted combustion gas systematically by using a high-speed camera, and this can infer the generation of thrust.

5.1. Ignition characteristic

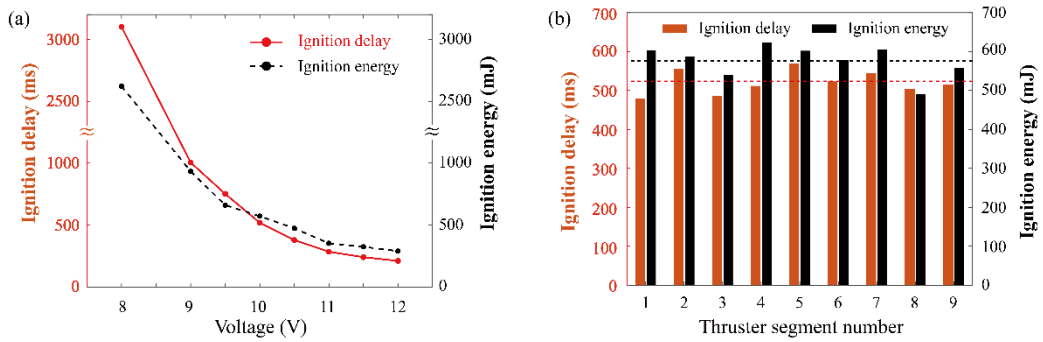

Fig. 10. (a) Ignition characteristic of the micro ignitor, (b) Ignition characteristics for the entire 3 × 3 SPMT array at 10 V.

The ignition delay and energy as a function of the applied voltage are shown in Fig. 10(a). For each point, we repeated the experiments three times. Below 7.9 V, combustion was not initiated even with a prolonged supply of electricity. The ignition delay and energy decreased exponentially as the input voltage increased[48]. The maximum ignition delay was 3.10 s at the input voltage of 8 V, and the minimum was 211.85 ms at the input voltage of 12V, where the ignition energy was measured to be 290.58 mJ. Furthermore, when a voltage of 12.1 V or higher was applied, the coated ignitor was fractured, resulting in a failure. We expected that the micro ignitors can have a reduced ignition delay and energy if using conductive paste with higher heat resistance. Figure 10b shows the ignition delay and energy when each segment of the SPMT array was sequentially ignited at 10 V for reliability evaluation. The average ignition delay (red dotted line) and energy (black dotted line) of the 9 thruster segments were 521.17 ms and 576.74 mJ, respectively, with standard deviations of 30.77 ms and 41.14 mJ. This result suggests that the igniter has favorable reliability and reproducibility.

The direct contact of the ignitor, which was used in our research, allowed a fairly lower value of the ignition delay and ignition energy. Compare to AP/HTPB propellant, which has similar combustion characteristics to ours, it has a significantly larger value of the ignition delay and energy, 1.6 s and 1.43 J, respectively, at 12 V[50]. This demonstrates that the micro ignitor fabricated in this study shows strengths the ones of previous studies not only in terms of benefits in the manufacturing process for mass production and upscaling but also for performance.

5.2. Thruster propulsion validation

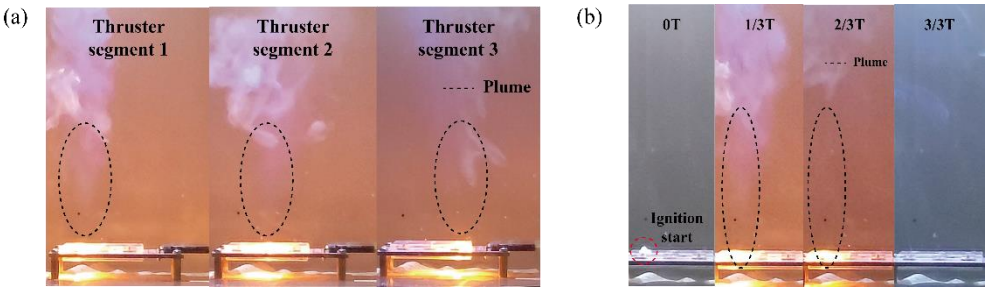

Fig. 11. (a) Combustion in different thruster segments of SPMT, (b) Time-sequential combustion images for AP/PDMS propellant

Figure 11 depicts the combustion of the AP-PDMS propellant. Images were acquired at 960 fps. A total of 9 thruster segments were used to measure thrust, and all segments were successfully ignited to generate thrust. Sequential combustion of thruster segments at different positions was initiated with

the coated ignitors (Fig. 11a), and the combustion process was captured with a high-speed camera (Fig. 11b). In Fig. 11b, the combustion duration was divided into thirds with photos of the combustion at each time point. A plume generated by gas ejection can be seen in the area inside the black dotted line. A clear plume forms due to the low smoke characteristics of the propellant, and vivid white gas is produced during the early phases of ignition by the combustion of ignitor material, carbon paste.

6. 결 론

In this study, we designed and fabricated a 3 × 3 SPMT array based on the lab-on-PCB concept. We conducted a number of tests to check the process's feasibility and confirmed its potential to be expanded for mass production and upscaling. AP/PDMS solid propellants and ignitors were installed to the PCB with incorporated combustion chamber array specially designed to create an on-board thruster. As an effort to improve the process and ease of control, the PCB contained embedded circuitry and electrodes that were connected to ignitor precursors by a coating process. We chose the silkscreening method for fast and accurate insertion of the solid propellant precursor into the board. Conductive paste was used for the ignitor precursor, and it was applied onto the propellant by the bar-coating method. These methods share the properties of having high reliability and fast processing time and are therefore favorable for mass production and upscaling. The nozzle array was fabricated using an attosecond pulse laser, which is more precise and faster than conventional etching methods. All components were made out of polycarbonate or FR-4, resulting in improved robustness compared to silicon or glass-based thrusters. The resistance of the micro ignitor array set made by coating measured relatively uniform resistances, with an average value of 94.15 Ω and a standard deviation of 3.68 Ω. In the ignition tests, all of the propellants were successfully ignited, and the minimum energy for ignition was measured to be 290.58 mJ with an ignition delay of 211.85 ms. Compared to other thrusters using propellants with similar combustion properties, our thruster demonstrated better ignition characteristics. The thrust generation was observed for all thruster segments of a 3 × 3 SPMT array. We demonstrated a new fabrication process of a fully functional SPMT array based on the lab-on-PCB concept. This can demonstrate the possibility of the propulsion system and the electronic control system of micro-satellite.

Such a device can be deemed not as a thruster but as a gas generator emitting a set amount of fluid using cartridge-type solid energetic materials. The total impulse from each segment being uniform implies the same for the emitted amount of gas. By applying this approach to the field of soft robotics, the chronic problem of difficulty in downsizing a fluid pump[51] could be overcome. Also, this approach is more competent for downsizing compared to conventional fluid pumps using gas combustions[52-54]. Outside space applications, our results suggest its potential as an actuator in multiple fields.

참고문헌

[1] I. Levchenko et al., "Space micropropulsion systems for Cubesats and small satellites: From proximate targets to furthermost frontiers," Applied Physics Reviews, vol. 5, no. 1, p. 011104, Feb 2018.
[2] B. Lal et al., Global trends in small satellites. JSTOR, Feb 2017.
[3] M. Sweeting, "Modern small satellites-changing the economics of space," Proceedings of the IEEE, vol. 106, no. 3, pp. 343-361, Feb 2018.
[4] S. Bandyopadhyay, R. Foust, G. P. Subramanian, S.-J. Chung, and F. Y. Hadaegh, "Review of formation flying and constellation missions using nanosatellites," Journal of Spacecraft and Rockets, vol. 53, no. 3, pp. 567-578, Mar 2016.
[5] R. Sandau, "Status and trends of small satellite missions for Earth observation," Acta

Astronautica, vol. 66, no. 1–2, pp. 1–12, Feb 2010.
[6] P. G. Buzzi, D. Selva, N. Hitomi, and W. J. Blackwell, "Assessment of constellation designs for earth observation: Application to the TROPICS mission," Acta Astronautica, vol. 161, pp. 166–182, Aug 2019.
[7] W. W. Weiss et al., "BRITE-constellation: nanosatellites for precision photometry of bright stars," Publications of the Astronomical Society of the Pacific, vol. 126, no. 940, p. 573, Jun 2014.
[8] G. Curzi, D. Modenini, and P. Tortora, "Large constellations of small satellites: A survey of near future challenges and missions," Aerospace, vol. 7, no. 9, p. 133, Sep 2020.
[9] E. Gill, P. Sundaramoorthy, J. Bouwmeester, B. Zandbergen, and R. Reinhard, "Formation flying within a constellation of nano-satellites: The QB50 mission," Acta Astronautica, vol. 82, no. 1, pp. 110–117, Jan 2013.
[10] V. L. Foreman, A. Siddiqi, and O. De Weck, "Large satellite constellation orbital debris impacts: Case studies of oneweb and spacex proposals," in AIAA SPACE and Astronautics Forum and Exposition, Sep 2017, p. 5200.
[11] A. P. London, "A systems study of propulsion technologies for orbit and attitude control of microspacecraft," Massachusetts Institute of Technology, Jun 1996.
[12] N. Meckel, W. Hoskins, R. Cassady, R. Myers, S. Oleson, and M. McGuire, "Improved pulsed plasma thruster systems for satellite propulsion," in 32nd Joint Propulsion Conference and Exhibit, 1996, p. Jul 2735.
[13] M. A. Silva, D. C. Guerrieri, A. Cervone, and E. Gill, "A review of MEMS micropropulsion technologies for CubeSats and PocketQubes," Acta Astronautica, vol. 143, pp. 234–243, Feb 2018.
[14] D. Scharfe and A. Ketsdever, "A review of high thrust, high delta-V options for microsatellite missions," in 45th AIAA/ASME/SAE/ASEE Joint Propulsion Conference & Exhibit, p. 4824, Jun 2009.
[15] Kulu and Erik. "Nanosats database." https://www.nanosats.eu, 2022.
[16] B. Liu, X. Li, J. Yang, and G. Gao, "Recent advances in MEMS-based microthrusters," Micromachines, vol. 10, no. 12, p. 818, Nov 2019.
[17] J. Köhler et al., "A hybrid cold gas microthruster system for spacecraft," Sensors and Actuators A: Physical, vol. 97, pp. 587–598, Apr 2002.
[18] R. Ranjan, K. Karthikeyan, F. Riaz, and S. Chou, "Cold gas propulsion microthruster for feed gas utilization in micro satellites," Applied Energy, vol. 220, pp. 921–933, Jun 2018.
[19] P. Kundu, A. K. Sinha, T. K. Bhattacharyya, and S. Das, "MnO2 Nanowire Embedded Hydrogen Peroxide Monopropellant MEMS Thruster," Journal of Microelectromechanical Systems, vol. 22, no. 2, pp. 406–417, Apr 2013.
[20] J. Huh and S. Kwon, "Design, fabrication and thrust measurement of a micro liquid monopropellant thruster," Journal of Micromechanics and Microengineering, vol. 24, no. 10, p. 104001, Sep 2014.
[21] J. Huh, D. Seo, and S. Kwon, "Fabrication of a liquid monopropellant microthruster with built-in regenerative micro-cooling channels," Sensors and Actuators A: Physical, vol. 263, pp. 332–340, Aug 2017.
[22] A. London et al., "Microfabrication of a high pressure bipropellant rocket engine," Sensors and Actuators A: Physical, vol. 92, no. 1–3, pp. 351–357, Aug 2001.
[23] M.-H. Wu and P.-S. Lin, "Design, fabrication and characterization of a low-temperature co-fired ceramic gaseous bi-propellant microthruster," Journal of Micromechanics and Microengineering, vol. 20, no. 8, p. 085026, Jul 2010.
[24] A. Cervone, B. Zandbergen, D. C. Guerrieri, M. De Athayde Costa e Silva, I. Krusharev, and H. Van Zeijl, "Green micro-resistojet research at Delft University of Technology: new options for Cubesat propulsion," CEAS Space Journal, vol. 9, no. 1, pp. 111–125, Jul 2016.
[25] A. Greig, C. Charles, N. Paulin, and R. Boswell, "Volume and surface propellant heating in an

electrothermal radio-frequency plasma micro-thruster," Applied Physics Letters, vol. 105, no. 5, p. 054102, 2014.
[26] C. Charles, R. Boswell, and A. Bish, "Low-weight fixed ceramic capacitor impedance matching system for an electrothermal plasma microthruster," Journal of Propulsion and Power, vol. 30, no. 4, pp. 1117-1121, Aug 2014.
[27] S. P. Berg, J. Rovey, B. Prince, S. Miller, and R. Bemish, "Electrospray of an energetic ionic liquid monopropellant for multi-mode micropropulsion applications," in 51st AIAA/SAE/ASEE Joint Propulsion Conference, p. 4011, Jul 2015.
[28] J. Xiong, Z. Zhou, D. Sun, and X. Ye, "Development of a MEMS based colloid thruster with sandwich structure," Sensors and Actuators A: Physical, vol. 117, no. 1, pp. 168-172, Jan 2005.
[29] D. H. Lewis Jr, S. W. Janson, R. B. Cohen, and E. K. Antonsson, "Digital micropropulsion," Sensors and Actuators A: Physical, vol. 80, no. 2, pp. 143-154, Mar 2000.
[30] D. Seo, J. Jeong, T. Kim, and J. Lee, "A MEMS glass membrane igniter for improved ignition delay and reproducibility," Sensors and Actuators A: Physical, vol. 258, pp. 22-31, May 2017.
[31] X. Liu, T. Li, Z. Li, H. Ma, and S. Fang, "Design, fabrication and test of a solid propellant microthruster array by conventional precision machining," Sensors and Actuators A: Physical, vol. 236, pp. 214-227, Dec 2015.
[32] C. Rossi, S. Orieux, B. Larangot, T. Do Conto, and D. Esteve, "Design, fabrication and modeling of solid propellant microrocket-application to micropropulsion," Sensors and Actuators A: Physical, vol. 99, no. 1-2, pp. 125-133, Apr 2002.
[33] C. Rossi, B. Larangot, D. Lagrange, and A. Chaalane, "Final characterizations of MEMS-based pyrotechnical microthrusters," Sensors and Actuators A: Physical, vol. 121, no. 2, pp. 508-514, Jun 2005.
[34] S. Tanaka et al., "Test of B/Ti multilayer reactive igniters for a micro solid rocket array thruster," Sensors and Actuators A: Physical, vol. 144, no. 2, pp. 361-366, Jun 2008.
[35] J. Lee and T. Kim, "MEMS solid propellant thruster array with micro membrane igniter," Sensors and Actuators A: Physical, vol. 190, pp. 52-60, Feb 2013.
[36] J. Lee, K. Kim, and S. Kwon, "Design, fabrication, and testing of MEMS solid propellant thruster array chip on glass wafer," Sensors and Actuators A: Physical, vol. 157, no. 1, pp. 126-134, Jan 2010.
[37] D. Seo, J. Lee, and S. Kwon, "The development of the micro-solid propellant thruster array with improved repeatability," Journal of Micromechanics and Microengineering, vol. 22, no. 9, p. 094004, Aug 2012.
[38] F. Perdigones, "Lab-on-PCB and flow driving: A critical review," Micromachines, vol. 12, no. 2, p. 175, Feb 2021.
[39] M.-H. Wu and R. A. Yetter, "A novel electrolytic ignition monopropellant microthruster based on low temperature co-fired ceramic tape technology," Lab on a Chip, vol. 9, no. 7, pp. 910-916, Dec 2008.
[40] D. Moschou and A. Tserepi, "The lab-on-PCB approach: tackling the μTAS commercial upscaling bottleneck," Lab on a Chip, vol. 17, no. 8, pp. 1388-1405, Mar 2017.
[41] W. Zhao, S. Tian, L. Huang, K. Liu, and L. Dong, "The review of Lab-on-PCB for biomedical application," Electrophoresis, vol. 41, no. 16-17, pp. 1433-1445, Jan 2020.
[42] R. H. Liu, J. Yang, R. Lenigk, J. Bonanno, and P. Grodzinski, "Self-contained, fully integrated biochip for sample preparation, polymerase chain reaction amplification, and DNA microarray detection," Analytical chemistry, vol. 76, no. 7, pp. 1824-1831, Feb 2004.
[43] M. Boyd-Moss, S. Baratchi, M. Di Venere, and K. Khoshmanesh, "Self-contained microfluidic systems: a review," Lab on a Chip, vol. 16, no. 17, pp. 3177-3192, Jul 2016.
[44] G. F. Salado, "Self-contained microfluidic platform for general purpose lab-on-chip using pcb-mems technology," Universidad de Sevilla, 2017.
[45] A. Chaalane et al., "A MEMS-based solid propellant microthruster array for space and military applications," in Journal of Physics: Conference Series, vol. 660, no. 1: IOP Publishing, p.

012137, 2015.
[46] K. Zhang, S. Chou, and S. S. Ang, "Development of a solid propellant microthruster with chamber and nozzle etched on a wafer surface," Journal of Micromechanics and Microengineering, vol. 14, no. 6, p. 785, Apr 2004.
[47] C. Rossi, D. Briand, M. Dumonteuil, T. Camps, P. Q. Pham, and N. F. De Rooij, "Matrix of 10×10 addressed solid propellant microthrusters: Review of the technologies," Sensors and Actuators A: Physical, vol. 126, no. 1, pp. 241-252, Jan 2006.
[48] C. Rossi, P. Temple-Boyer, and D. Estève, "Realization and performance of thin SiO2/SiNx membrane for microheater applications," Sensors and Actuators A: Physical, vol. 64, no. 3, pp. 241-245, Jan 1998.
[49] K. Zhang, S. Chou, and S. Ang, "Fabrication, modeling and testing of a thin film Au/Ti microheater," International Journal of Thermal Sciences, vol. 46, no. 6, pp. 580-588, Jun 2007.
[50] J. Lee, "Internal ballistic design and fabrication procedure of MEMS solid propellant rocket," ed: KAIST, 2009.
[51] G. Zhang et al., "A Pneumatic Generator Based on Gas-Liquid Reversible Transition for Soft Robots," in Actuators, vol. 10, no. 5: MDPI, p. 103, May 2021.
[52] M. Wehner et al., "An integrated design and fabrication strategy for entirely soft, autonomous robots," nature, vol. 536, no. 7617, pp. 451-455, Aug 2016.
[53] N. W. Bartlett et al., "A 3D-printed, functionally graded soft robot powered by combustion," Science, vol. 349, no. 6244, pp. 161-165, Jul 2015.
[54] R. F. Shepherd et al., "Using explosions to power a soft robot," Angewandte Chemie International Edition, vol. 52, no. 10, pp. 2892-2896, Feb 2013.